Applied Acoustics 185 (2022) 108426

Contents lists available at ScienceDirect

Applied Acoustics

journal homepage: www.elsevier.com/locate/apacoust

# Statistical analysis of sound level predictions in refracting and turbulent atmospheres

Timothy Van Renterghem [a,*], Kirill V. Horoshenkov [b], Jordan A. Parry [c], Duncan P. Williams [d]

[a] Ghent University, Department of Information Technology, WAVES Research Group, Technologiepark 126, B 9052 Gent-Zwijnaarde, Belgium
[b] University of Sheffield, Department of Mechanical Engineering, Sheffield S1 3JD, UK
[c] JaGNum Ltd, Doncaster, England
[d] Defence Science and Technology Laboratory, Salisbury, England

ARTICLE INFO

*Article history:*
Received 1 June 2021
Received in revised form 10 September 2021
Accepted 13 September 2021

*Keywords:*
Outdoor sound propagation
Atmospheric refraction
Turbulent scattering
Uncertainty

ABSTRACT

There is a lack of data on the statistical properties of the sound pressure level fluctuations which are caused by uncertainties in source/receiver heights, range, ground conditions and atmospheric effects. This paper contributes to this knowledge gap through statistical analysis of the atmospheric effects on sound pressure levels performed with a Green's function parabolic equation model and a turbulence scattering model. The probability density functions for the sound pressure level relative to free field propagation are calculated for the source and receiver close to the ground, up to 1 km propagation distance, for typical annual meteorological conditions and two types of ground. It is found that the ground type and refractive state of the atmosphere have a pronounced effect on the probability distribution. Under some conditions and at some frequency intervals, distributions can be remarkably similar. Furthermore, accounting for meteorological effects become increasingly important with range when predicting sound pressure level distributions. This work contributes to a better understanding of the role of uncertainties in outdoor sound propagation that might serve for improved accuracy of statistical source localisation and characterisation methods based on parameter inversion.



## 1. Introduction

There has been works on uncertainties in outdoor sound propagation which suggest that they are significantly affected by the ground effect, source and receiver height, range and atmospheric conditions. The effects of these uncertainties are described in Ref. [1]. More recent works attempted to quantify the important role of uncertainties in outdoor sound propagation prediction and described a variety of methods for quantifying the impacts of these uncertainties [2]. However, there is still a lack of statistical data obtained via simulation [3] or experimental work [4]. Although more work has been done through numerical simulations to study the effect of uncertainties on sound propagation in a non-moving homogeneous atmosphere over an impedance ground [5], there are still open questions remaining to be answered.

These questions are: *(i) When does it make sense to use complex prediction models to obtain accurate statistics which account for atmospheric effects? (ii) Are there some atmospheric conditions when the uncertainty is too great to capture acoustic data accurately with a complex prediction model? (iii) Which are the key parameters dominating the uncertainty in the predicted sound pressure level?*

This paper attempts to answer the above questions using the Green's function parabolic equation (GFPE) model [6] which is combined with an engineering turbulence model to determine the probability density functions for the sound pressure levels relative to free field sound propagation, determined for a representative range of geometrical, ground and atmospheric conditions. Coupling outdoor sound propagation models with detailed weather data has been performed before [7–9], but not for the specific purpose of drawing probability density functions. These results will be compared with those obtained for a still and homogeneous atmosphere, i.e. the instance which it is easy to predict with a relatively simple and very computationally efficient model [5].

A key motivation for this work is the source localization in the presence of meteorological and ground uncertainties. There are a number of applications for this work. Gun detection is of obvious importance in defence applications, yet it is still an understudied area particularly in the case of large-scale outdoor situations. Another application is the localization of industrial sources of environmental noise particular those which bring annoyance into adja-

* Corresponding author.
*E-mail address:* timothy.vanrenterghem@ugent.be (T. Van Renterghem).

https://doi.org/10.1016/j.apacoust.2021.108426
0003-682X/

cent residential areas. There is also a clear need to separate sources of sounds to understand and to design positive soundscapes in outdoor environments. All these applications require good understanding of the potential for the sound pressure level variability across the spectrum of audible frequencies and its relation to the uncertainties in the propagation path.

This paper is organised in the following manner. Section 2 details the research methodology, the numerical model and the meteorological data that was used. Section 3 describes the results. Section 4 summarises the findings of this study.

## 2. Research methods

Data on the atmospheric conditions used in this work are based on historical weather information collected from a meteorological tower near the city of Mol, in Belgium, for the year 1997. The meteorological data contains 10-minute averages of wind speed (at 24 m, 48 m, 69 m, 78 m, and 114 m above the ground) and air temperature (8 m, 24 m, 48 m, 78 m, and 114 m). Sound propagation in the dominant downwind direction was considered.

Only 10-minute averaged data with complete meteorological observations were used, which was 77.5% of the total number of records in the dataset. From this dataset 1000 cases were randomly drawn without replication (see Fig. 1). The height-dependent effective sound speed $c_{eff}$ was then calculated using air temperature, wind speed and wind direction:

$$c_{eff}(z) = \sqrt{\kappa R T(z)} + u_{SR}(z), \quad (1)$$

with $z$ the height above the ground, $\kappa$ is the ratio of the specific heat capacities at constant pressure and constant volume (which is 1.4 for air), $R$ is the gas constant of dry air (287 J/(kg K)) and $T(z)$ is the height-dependent air temperature. The wind speed profile along the source-receiver line is given by $u_{SR}(z)$, and has a positive sign for downwind propagation, a negative sign for upwind propagation, and becomes zero in case of cross-wind.

A linear-logarithmical (effective) sound speed curve was fitted on the measured data:

$$c_{eff} = a_0 + a_{lin} z + a_{\log} \log\left(\frac{z + z_0}{z_0}\right). \quad (2)$$

Parameter $a_0$ is the sound speed $(\mathrm{ms}^{-1})$ at $z$ = 0 m, the coefficients $a_{lin}$ and $a_{log}$ can be related to the physical parameters of theoretical-empirical flux-profile relationships for flat and homogeneous terrain [10]. This type of profile as in eq. (2) was found to provide very good fits on meteorological tower data [9,11]. A roughness height of $z_0$ = 0.2 m is appropriate for the surroundings of the meteorological tower.

The coefficients $a_{lin}$ and $a_{log}$ in eq. (2) were obtained by fitting the meteorological observations. The values of these coefficients used in this study are shown as the smaller circles in Fig. 1. Sound propagation from a point source under these meteorological conditions over flat ground was simulated with the 2D axi-symmetric GFPE, a well-established directional wave-based model, accounting in high detail for refracting atmospheres in the presence of an impedance ground plane. Detailed information on the model, parameter settings and example applications can be found elsewhere [6,9,12].

For the simulations presented in this paper, a range-independent sound speed profile and a range-independent ground impedance was considered to predict $SPL_{reFF,nosc}$, which is the sound pressure level relative to free field propagation accounting for the presence of refraction and ground, but in absence of turbulent scattering. This indicator is the negative of the so-called "excess attenuation" [1]. In the case of upward refracting atmospheres, or when pronounced destructive interference dips in the sound pressure level spectra are predicted, unrealistic low sound pressure levels are usually obtained when neglecting scattering by a turbulent atmosphere. Based solely on the previously described meteorological tower data, by using horizontal wind speed and air temperature profiles, estimating the turbulent state of the atmosphere becomes unreliable. Therefore, the ERA5 database [13] was consulted, providing hourly predictions of a wide range of atmospheric parameters allowing estimates of the turbulence strength. This so-called re-analysis data is available at a spatial resolution of 30 km by 30 km. The closest point to the tower was consequently selected. From this database, the surface heat flux $Q_H$, surface temperature $T_s$ and friction velocity $u_*$ were retrieved at the corresponding moments of the 1000 draws from the meteorological tower measurements. These parameters allow calculating the Monin-Obhukov length $L_{MO}$ [14]:

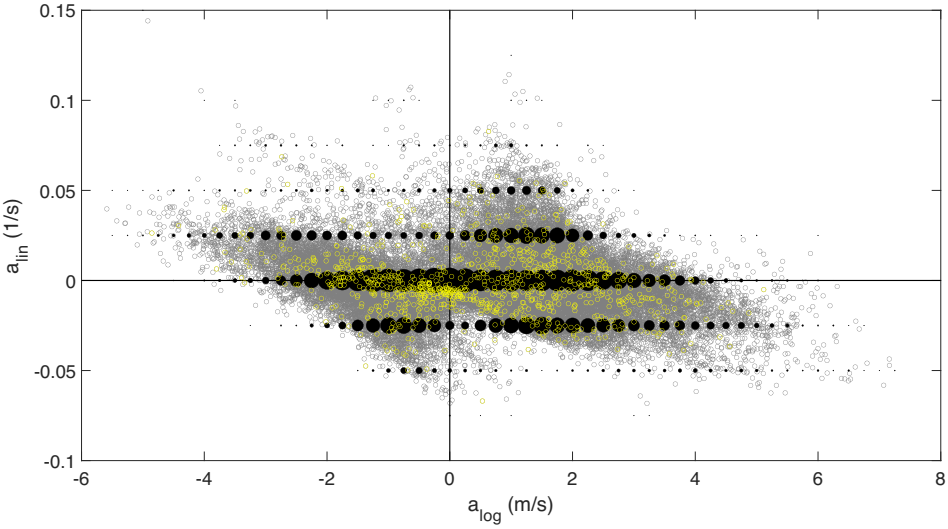


**Fig. 1.** Scatter plot of the coefficients $a_{log}$ against $a_{lin}$ for experimentally collected data (grey open circles) of size $N = 40740$. It is used to select 1000 data points (yellow circles) to run GFPE simulations. The black filled circles represent the classified $a_{log}$-$a_{lin}$ pairs, where the radius is proportional to the occurrence in each class. (For interpretation of the references to colour in this figure legend, the reader is referred to the web version of this article.)

$$L_{MO} = -\frac{u_*^3 T_s \rho_0 c_p}{g k_v Q_H}, \tag{3}$$

where $g$ is the gravitational acceleration (9.81 m/s$^2$), $c_P$ is the heat capacity of air at constant pressure (1000 J/kg), $\rho_0$ is the density of air (1.2 kg/m$^3$), and $k_v$ the von Karman constant for air (0.4).

The temperature scale $T_*$ can be calculated as follows [14]:

$$T_* = -\frac{Q_H}{u_* \rho_0 c_p}. \tag{4}$$

In the atmospheric surface layer, air temperature fluctuations can be described by its variance $\sigma_T^2$ and related length scale $L_T$, using following empirical expressions [14,15]:

$$\sigma_T^2(z) = T_*^2 \frac{4}{\left[1 + 10\left(-\frac{z}{L_{MO}}\right)\right]^{\frac{2}{3}}}, \tag{5}$$

$$L_T(z) = 2z \frac{\left[1 + 7\left(-\frac{z}{L_{MO}}\right)\right]}{\left[1 + 10\left(-\frac{z}{L_{MO}}\right)\right]}. \tag{6}$$

In case of shear dominated surface layer turbulence, the variance of the horizontal component of the wind speed $\sigma_v^2$ and its length scale $L_v$ can be approached as follows [14]:

$$\sigma_v^2(z) = 3u_*^2, \tag{7}$$

$$L_v(z) = 1.8z. \tag{8}$$

Equations (5)–(8) allow estimating the so-called structure parameters for temperature ($C_T^2$) and velocity ($C_v^2$) using Kolmogorov's statistical representation of a turbulent atmosphere in the inertial subrange [14]:

$$C_T^2 = \frac{3\Gamma\left(\frac{5}{6}\right)}{\pi^{\frac{1}{2}}} \frac{\sigma_T^2}{L_T^{\frac{2}{3}}}, \tag{9}$$

$$C_v^2 = \frac{3\Gamma\left(\frac{5}{6}\right)}{\pi^{\frac{1}{2}}} \frac{\sigma_v^2}{L_v^{\frac{2}{3}}}, \tag{10}$$

where $\Gamma$ denotes the gamma function. For a more complete description of the theoretical and empirical equations shown above, including their validity ranges, the reader is referred to Ref. [14].

Although the GFPE model allows for explicitly modelling turbulent realisations by perturbing sound speed profiles [6], a large number of such realisations (typically at least 30–50) are needed to end up with energetically averaged and converged levels, blowing up computational efforts.

Instead, it was chosen to correct the sound pressure levels in a refracting atmosphere that neglect turbulent scattering. One possibility is to add a scattering contribution [16,17]:

$$SPL_{reFF,sc} = 25 + 10\log_{10}\gamma_T + 3\log_{10}\frac{\omega}{1000} + 10\log_{10}\frac{d}{100}, \tag{11}$$

where $\omega$ is sound frequency, $d$ is the source-receiver separation, and $\gamma_T$ is a measure of the turbulence strength. The latter is a combination of the structure parameters predicted by Eq. (9) and Eq. (10):

$$\gamma_T = \left(\frac{C_T}{T_0}\right)^2 + \frac{22}{3}\left(\frac{C_v}{c_0}\right)^2. \tag{12}$$

Finally, the sound pressure levels relative to free field in a refracting atmosphere can be corrected for turbulent scattering in the following way:

$$SPL_{reFF} = 10\log_{10}\left(10^{\frac{SPL_{reFF,nosc}}{10}} + 10^{\frac{SPL_{reFF,sc}}{10}}\right). \tag{13}$$

The above equations enabled us to simplify the highly complex case of scattering of sound by a turbulent atmosphere and to moderate unrealistically low levels of the sound pressure level, $SPL_{reFF,nosc}$. At the same time, the temporal variation in atmospheric turbulence strength and its link with the sound speed profile (see Eq. (2)) is kept. Given the different time scales of data availability, successive 10-minute sound speed profiles will be assigned the same hourly turbulent scattering strength.

Although the Kolmogorov model assumes isotropic and statistically homogeneous turbulence [14], spatially coarse atmospheric turbulence parameters were used [13], and an engineering turbulent scattering model was used [16,17], it allows to at least discriminate between atmospheres with weak and strong turbulent scattering. This potentially has a significant influence on the tails of the sound pressure level distributions.

Figs. 2 and 3, as an example, show the sound pressure level spectra predicted with eq. (13) for strong and weak turbulence scattering, respectively. The predictions without scattering, $SPL_{reFF,nosc}$, are depicted as well. The simulations agree with experimental findings and other numerical approaches showing a more or less range independent level when expressing sound pressure levels relative to free field sound propagation under upwardly refracting conditions [18–21].

These figures illustrate three important points: (i) the sound pressure level relative to the free field predicted by the GFPE model scattering is unlikely to fall below −30dB[1]; (ii) weak turbulence scattering can be neglected for lower frequencies of sound and short/medium range; (iii) strong turbulent conditions might lead to a level increase of up to 20 dB when compared to weakly scattering atmospheres.

## 3. Results

To generate the probability density functions (PDFs from hereon) required, we need repeated simulations using the GFPE model. Each simulation is run over a given set of parameters (see Fig. 1), with each resulting value (see eq. (13)) being recorded. These values are then plotted against their respective probabilities i.e. the probability of achieving a given value across all the possible combinations of parameters.

For the parameters in question for this study, the impedance ground remains flat, with acoustical hardness representing a softer grassland $\left(\sigma_g = 100\text{kPasm}^{-2}\right)$ or harder rocky terrain $\left(\sigma_g = 2000\text{kPasm}^{-2}\right)$ matching their experimental results [1]. The ground impedance is calculated via the effective flow resistivity $\sigma_g$ using an experimentally proven model proposed by Horoshenkov et al [22]. This model has been reliably applied in previous related statistical studies [5].

The range $r$ is from 100 to 1000 m. The (point) source height $h_s$ is at 2 m while the receiver height $h_r$ is allowed to take values up to 15 m high. Calculations were performed for 1/3 octave bands, which will be indicated by their centre frequencies, ranging from 100 Hz to 2500 Hz. Fifteen individual frequencies were considered to constitute each 1/3 octave band response. For brevity we present only data for $h_r = 1.55$ m in this paper. A full set of the results for this and other receiver heights can be found as supplementary material available online [23].

### 3.1. No meteorological effects

As previously shown by Parry and Horoshenkov [5], the interference patterns of outdoor sound propagation can be characterised using their statistical representation rather than the traditional sound pressure level spectrum. Fig. 4 shows the proba-

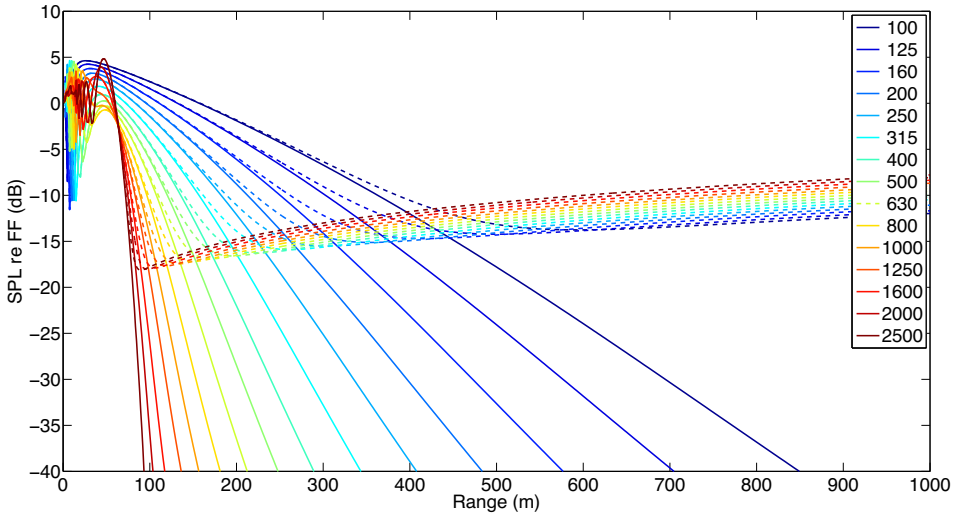


**Fig. 2.** The sound pressure level, relative to free field sound propagation, in an upward refracting atmosphere, predicted with eq. (13) for the 1/3 octave bands and receiver height of 2 m above the ground (grassland). Solid lines neglect turbulent scattering. Dashed lines are predictions corrected for strong turbulent scattering ($\gamma_T = 4.01 \times 10^{-5}, a_{log} = -1.1813 ms^{-1}$ and $a_{lin} = -0.0025 s^{-1}$).

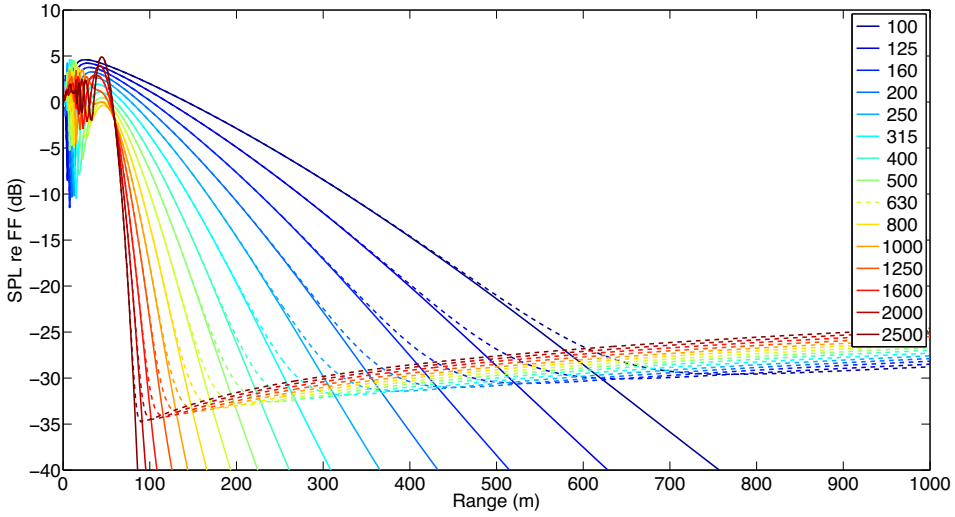


**Fig. 3.** The sound pressure level, relative to free field sound propagation, in an upward refracting atmosphere, predicted with eq. (13) for 1/3 octave bands and receiver height of 2 m above the ground (grassland). Solid lines neglect turbulent scattering. Dashed lines are predictions corrected for weak turbulent scattering ($\gamma_T = 8.51 \times 10^{-7}, a_{log} = -1.3323 ms^{-1}$ and $a_{lin} = -0.0005 s^{-1}$).

bility density function (PDF) for the sound pressure level (eq. (13)) predicted for the case without any atmospheric effects (so for a homogeneous, non-moving and non-turbulent atmosphere). The PDFs shown in Fig. 4 combine the statistics predicted for all the adopted ranges (100 – 1000 m). The results are separated for relatively soft and hard impedance grounds.

The results suggest that in the absence of any atmospheric effects the frequency is the dominant parameter that controls the PDFs. For this relatively low receiver height (1.55 m) and when going from a more rigid to a softer ground, the shape of the PDF does not change significantly, except for the bands where conditions for destructive interference are met (more precisely in the range 200–315 Hz in the current geometry). At even lower frequencies, distributions are not at all influenced by ground type. At higher frequencies, some very small shifts towards higher levels in the distributions are predicted, while their shapes are fully preserved, when going from rigid to soft grounds. Generally, the presence of the harder ground and higher receivers (not shown) result in a narrower sound pressure level range covered by the PDFs.

### 3.2. With meteorological effects

Fig. 1 separates the sound speed profiles into the four quadrants which correspond to four combinations of positive or negative values of the two coefficients in eq. (2). The sign of the coefficient $a_{log}$ primarily determines whether the sound propagation is downward refracting ($a_{log} > 0$, sound speed increases with height) or upward refracting ($a_{log} < 0$, sound speed decreases with height). The parameter $a_{lin}$ is much less influential as it controls the finer features in the sound speed profile as a function of height (see Section 3.2.3).

#### 3.2.1. Full downward refraction ($a_{log} > 0, a_{lin} > 0$)

Fig. 5 presents the PDFs for $a_{log} > 0$ and $a_{lin} > 0$ for the cases of the hard and soft ground. This type of atmosphere supports relatively long-range sound propagation which is affected more strongly by the ground conditions and less by the turbulent scattering (see e.g. Ref. [1,6,14]).

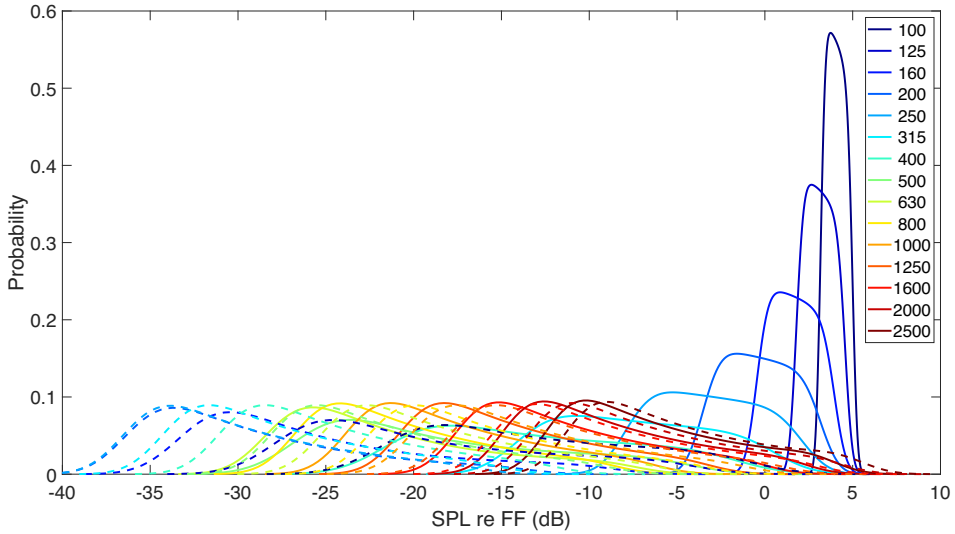


**Fig. 4.** The frequency dependence of the probability density function for the sound pressure levels relative to free field propagation excluding meteorological effects. Two types of grounds are considered (solid lines – rigid ground, dotted lines – soft ground) for a receiver height of 1.55 m, and range from 100 to 1000 m. The colour corresponds to the 1/3-octave band centre frequencies.

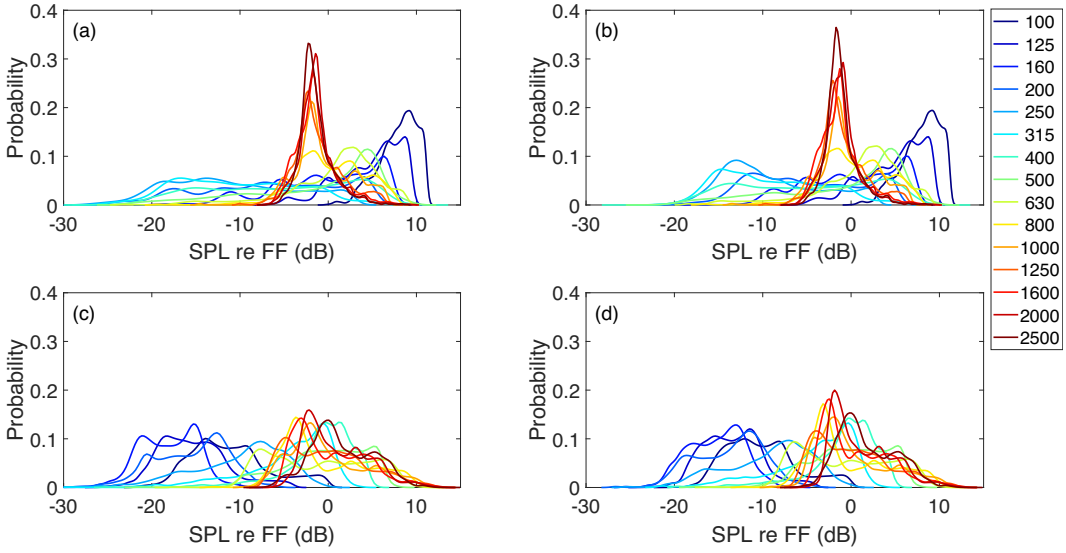


**Fig. 5.** The frequency dependence of the probability density function for the sound pressure levels, relative to free field propagation, for atmospheric conditions characterised with positive values (downward refraction) of $a_{log}$ and $a_{lin}$. In (a) and (b), rigid ground is considered; in (c) and (d) soft ground. In (a) and (c), turbulent scattering is neglected, while included in (b) and (d). Distributions are drawn for a fixed receiver height of 1.55 m, and range from 100 to 1000 m.

In case of downward refraction, complex interference patterns dominate at low frequencies (see Fig. 5). Localized zones with constructive and destructive interference lead to multi-peaked distributions when drawing along a line at constant height. In the case of rigid ground and frequencies below 500 Hz, these distributions are broad. In the case of very low frequencies, e.g. below 250 Hz, these distributions peak near +10 dB. This is due to constructive interference of multiple sound paths arriving at a single spot, enabling the predicted sound pressure level relative to free field to exceed 6 dB as would be expected in the case of a non-refracting atmosphere. At the higher frequencies, more peaked distributions with a maximum near 0 dB are predicted. At the frequencies above 1000 Hz and in the presence of rigid ground a remarkably sharp peak in the distribution is observed near −1 dB. The position of this peak and its width does not change significantly as the frequency increases further.

In the presence of soft ground pronounced zones with destructive interference at very low frequencies (below 250 Hz) are observed. This is consistent with that expected in the case of a non-refracting atmosphere but to a lesser extent. The maximum in the probability density function shifts down to approximately −15 dB. At the higher frequencies, a peak in the distribution near 0 dB is still observed but becomes wider for this type of ground.

The effect of turbulent scattering is relatively small in the case of downward refraction, consistent with findings reported in Ref. [6]. The probability of $SPL_{reFF}$ being below −20 dB becomes negligible. Somewhat larger differences between scattering/no scattering are observed at the lower end of the low frequency distributions and in the presence of soft ground.

### 3.2.2. Full upward refraction ($a_{log} < 0, a_{lin} < 0$)

Sound propagation in the atmosphere with a negative $a_{log}$ is markedly different to the case with $a_{log} > 0$ in terms of the predicted PDFs as illustrated in Fig. 6. This atmosphere supports upward sound refraction, shorter range sound propagation and it

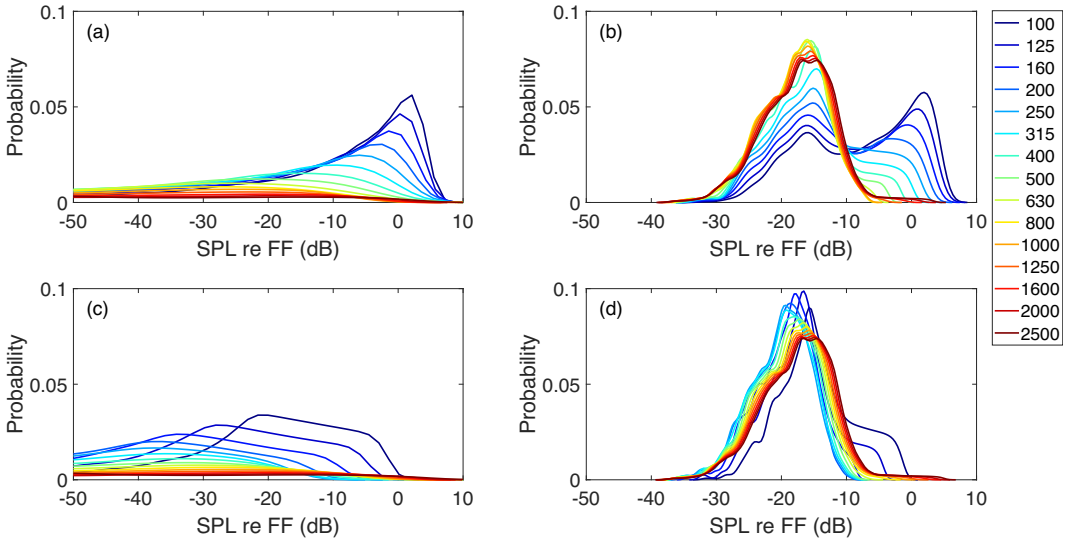


**Fig. 6.** The frequency dependence of the probability density function for the sound pressure levels, relative to free field propagation, for atmospheric conditions characterised with negative values (upward refraction) of $a_{log}$ and $a_{lin}$. In (a) and (b), rigid ground is considered; in (c) and (d) soft ground. In (a) and (c), turbulent scattering is neglected, while included in (b) and (d). Distributions are drawn for a fixed receiver height of 1.55 m, and range from 100 to 1000 m.

is affected strongly by the turbulent scattering and less by the ground conditions (see e.g. Ref. [1,6,14]).

In case of upward refraction and when neglecting turbulent scattering, a shadow zone can develop which effects become especially pronounced at low receiver heights (see e.g. Ref. [1,6,14]) as considered in this analysis. For very low frequencies and hard ground (see Fig. 6 (a)) a gradual transition between the insonified zone and the shadow zone is observed, extending over several hundred meters, leading to rather wide distributions. With increasing frequency, sound waves are more easily refracted, and the transition zone between insonified and shadow zone moves closer to the source. Relatively low values of the sound pressure level reflecting the presence of the close shadow zone are dominant in the PDFs drawn over all ranges as is done here.

At low frequencies and in the presence of rigid ground there is a maximum in the PDF around 0 dB (see Fig. 6 (a)) that is similar to the case of a non-refracting atmosphere. However, in the case of upward refraction (and still neglecting turbulent scattering) a tail is added to the distribution extending towards large negative values. This is a contribution from the acoustic shadow zone. In the presence of soft ground (see Fig. 6 (c)) the extensive low frequency destructive interference zone as observed in the case of a non-refracting atmosphere still plays an important role, shifting the PDFs to the lower levels.

When comparing simulation results with and without turbulent scattering, main differences are observed in the acoustic shadow zone. These extremely low sound pressure levels predicted with turbulent scattering being neglected fully disappear (see Fig. 6 (b) and (d)). The positive values of the sound pressure level relative to free field propagation, in contrast, are less affected by adding turbulent scattering to the simulations.

At sound frequencies above 500 Hz the probability density functions predicted with the turbulence scattering correction appear to be close to the Gaussian distribution with a maximum near −15/-20 dB (see Fig. 6 (b) and (d)). The shape of this distribution seems relatively independent of the ground type and frequency. The latter is particularly clear in the case of propagation above hard ground. Sound propagation in the presence of upward refraction is dominated by the turbulent scattering process, leading to values falling by and large between −30 dB (weak scattering episodes) and −10 dB (strong scattering episodes).

*3.2.3. Mixed sound speed profiles ($a_{log} > 0, a_{lin} < 0$ or $a_{log} < 0, a_{lin} > 0$)*

Sound propagation in atmospheres with mixed sound speed profiles give rather similar distributions as compared with the cases having consistently upward or downward refracting conditions (see Fig. 7). This means that that the sign of $a_{log}$ is the dominant factor governing the shape of the probability density functions.

A closer look at the graphs shows somewhat larger differences for low frequency 1/3 octave bands above rigid ground when $a_{log}$is negative (see Fig. 7 (b) as compared to Fig. 6 (b)). There, the bimodal behaviour as observed when $a_{lin}$ is negative is somewhat less pronounced.

### 3.3. Differences in statistics

It is of practical interest to quantify differences between the PDFs predicted for sound propagation either accounting for or neglecting meteorological influences. The question here is: *Starting from the non-refracting and non-turbulent atmosphere, when do we begin to observe significant changes in the probability density function upon adding results of simulations which include meteorological conditions defined by the coefficients $a_{log}$ and $a_{lin}$ (see Fig. 1) and the turbulence scattering term (see eq. (11))?* For this purpose, the degree of overlap of the surface below the PDFs accounting for or neglecting meteorological influence is calculated. As a criterion, we set the overlap threshold of 50%. If this threshold is exceeded, then the two PDFs are not very different, or the influence of the meteorological conditions we considered on sound propagation are not large. For these cases a simple and computationally efficient analytical model, e.g. van Der Pol [1,5], can be sufficient to estimate the statistical properties of the sound pressure level fluctuations caused by any uncertainties. Otherwise, a more complicated numerical model, e.g. GFPE [6], must be used. Note that calculation times with the GFPE model are easily a few orders of magnitude larger than when using an analytical approach neglecting meteorology.

*3.3.1. Effect of refraction type*

The above approach is applied separately for two quadrants for $a_{log}$ and $a_{lin}$ data as presented in Fig. 1. While adding to the statistics the results predicted for a new set of $a_{log}$ and $a_{lin}$ values we

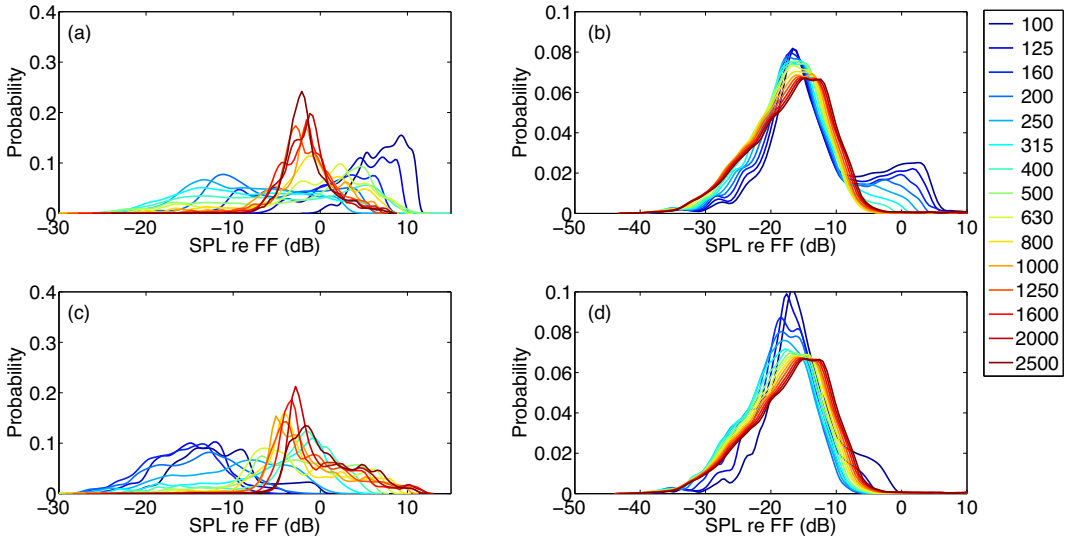


**Fig. 7.** The frequency dependence of the probability density function for the sound pressure levels, relative to free field propagation, for atmospheric conditions characterised with opposite values of $a_{log}$ and $a_{lin}$. In (a) and (b), rigid ground is considered; in (c) and (d) soft ground. In (a) and (c), $a_{log} > 0, a_{lin} < 0$, while in (b) and (d) $a_{log} < 0, a_{lin} > 0$. Turbulent scattering is included in all figures shown here. Distributions are drawn for a fixed receiver height of 1.55 m, and range from 100 to 1000 m.

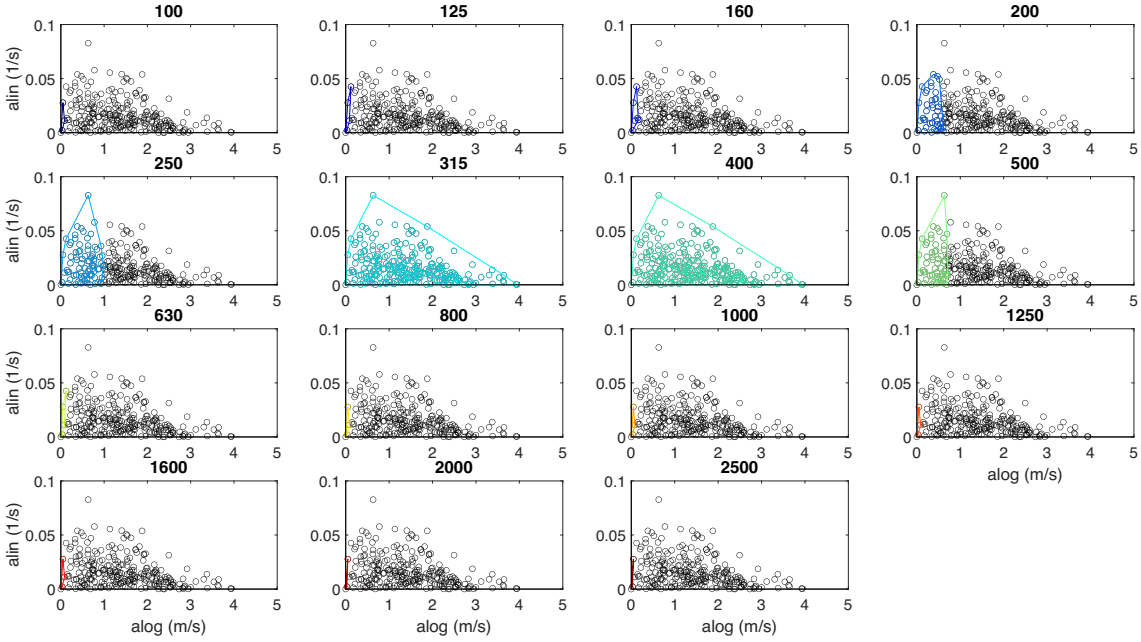


**Fig. 8.** The effect of downward refraction (positive values of $a_{log}$ and $a_{lin}$), including turbulent scattering, on the change in the probability density function of the sound pressure level relative to free field estimated in the presence of rigid ground, for the 1/3 octave bands with centre frequencies from 100 Hz to 2500 Hz. The coloured symbols indicate the range of $a_{log}$ values that can be included without leading to a less than 50% overlap in distribution relative to neglecting meteo. The colourmap is as in Fig. 4. The full receiver range from 100 m to 1000 m is included in this analysis, for a receiver height of 1.55 m.

always start with the lowest absolute values of $a_{log}$. Fig. 8 illustrates the results of this analysis for sound propagation under full downward refraction, i.e. when $a_{log} > 0$ and $a_{lin} > 0$, and in the presence of hard ground, including turbulent scattering. The extent of the quadrant covered by the coloured circles provides an estimate how much variability in the meteorological conditions need to be added to the model before the 'meteo' probability density function deviates too much (i.e. over 50 %) from that predicted for the 'no-meteo' case. The full range from 100 to 1000 m is included in this analysis.

These results show that for some 1/3 octave bands, e.g. 315 and 400 Hz, the difference threshold of 50% between the two cases is never reached, because it would require the addition of even more extreme $a_{log}$ conditions outside the range of those appearing in the yearly meteo tower dataset as used in this work (see Section 2). On the other hand, for all other bands a considerable difference occurs almost immediately upon adding the prediction made even for relatively small values of $a_{log}$ (e.g. 100 Hz graph in Fig. 8).

Fig. 9 is the counterpart of Fig. 8, but for sound propagation in the presence of soft ground. For almost any 1/3 octave band, a less

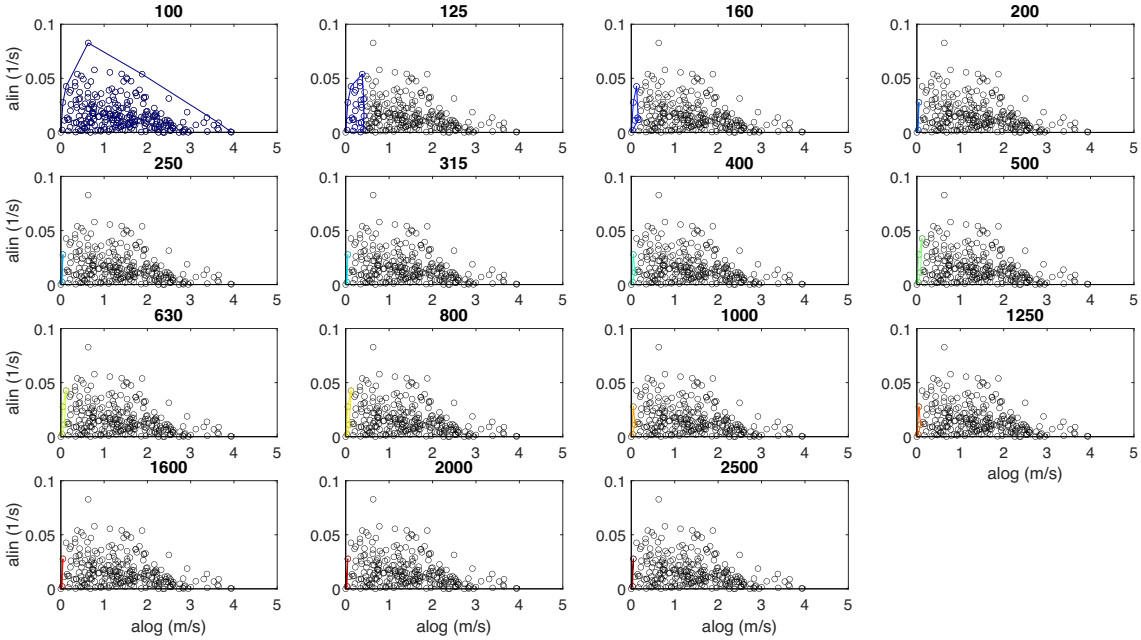


**Fig. 9.** The effect of downward refraction (positive values of $a_{log}$ and $a_{lin}$), including turbulent scattering, on the change in the probability density function of the sound pressure level relative to free field estimated in the presence of soft ground, for the 1/3 octave bands with centre frequencies from 100 Hz to 2500 Hz. The coloured symbols indicate the range of $a_{log}$ values that can be included without leading to a less than 50% overlap in distribution relative to neglecting meteo. The colourmap is as in Fig. 4. The full receiver range from 100 m to 1000 m is included in this analysis, for a receiver height of 1.55 m.

than 50% overlap in sound pressure level distribution (relative to neglecting meteorological influences) is rapidly reached upon adding the predictions made even for relatively small values of $a_{log}$. Only for the lowest frequency band of 100 Hz, less than 50% overlap is not reached.

In the case of upward refraction and hard ground, there are more similarities between the probability density functions predicted for the meteo and no-meteo cases. This is illustrated in Fig. 10 which shows that a more than 50% difference is never reached for sound propagation at the 1/3 octave bands with centre frequencies between 400 and 1600 Hz. For the frequencies of sound below and above this frequency range the PDFs diverge significantly with the increased value of $a_{log}$ relative to neglecting meteo.

These similarities between meteo/no-meteo are also pronounced in the case of sound propagation in upward refracting

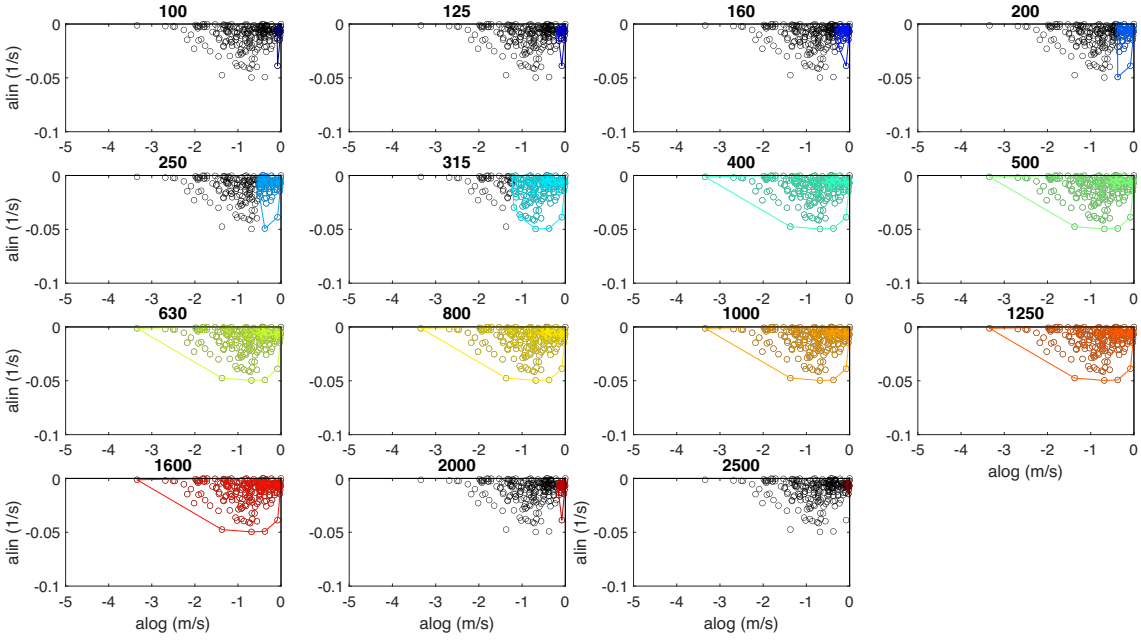


**Fig. 10.** The effect of upward refraction (negative values of $a_{log}$ and $a_{lin}$), including turbulent scattering, on the change in the probability density function of the sound pressure level relative to free field estimated in the presence of rigid ground, for the 1/3 octave bands with centre frequencies from 100 Hz to 2500 Hz. The coloured symbols indicate the range of $a_{log}$values that can be included without leading to a less than 50% overlap in distribution relative to neglecting meteo. The colourmap is as in Fig. 4. The full receiver range from 100 m to 1000 m is included in this analysis, for a receiver height of 1.55 m.

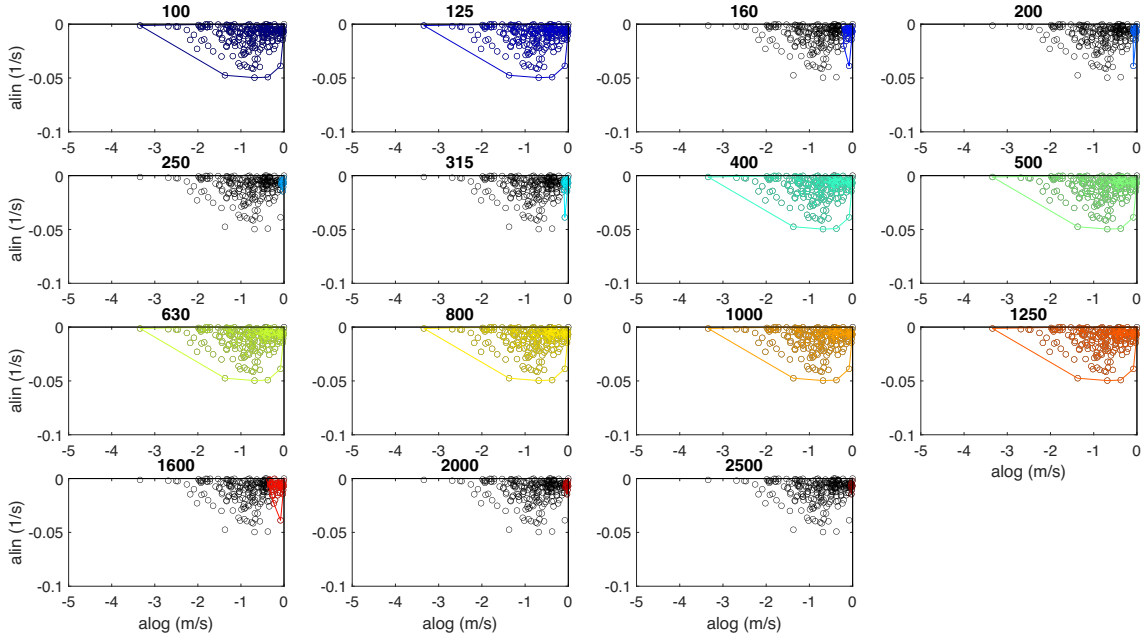


**Fig. 11.** The effect of upward refraction (negative values of $a_{log}$ and $a_{lin}$), including turbulent scattering, on the change in the probability density function of the sound pressure level relative to free field estimated in the presence of soft ground, for the 1/3 octave bands with centre frequencies from 100 Hz to 2500 Hz. The coloured symbols indicate the range of $a_{log}$ values that can be included without leading to a less than 50% overlap in distribution relative to neglecting meteo. The colourmap is as in Fig. 4. The full receiver range from 100 m to 1000 m is included in this analysis, for a receiver height of 1.55 m.

atmospheres in the presence of soft ground. This is illustrated in Fig. 11. For this case, the 50% difference threshold is never exceeded between the PDFs predicted at the frequencies below 125 Hz and in the range 400–1250 Hz.

### 3.3.2. Effect of range

Finally, it is of interest to study the effect of the range on the similarities between the probability density function of the sound pressure level relative to free field predicted with and without atmospheric effects. One can ask the following question: *Is there a certain range within which the presence of a non-uniform sound speed profile has little effect on the sound pressure level statistics?*

In this work the range-dependent similarity between the 'no meteo case' and 'meteo case' is estimated from the analysis of the corresponding PDFs which provided us with a fraction of overlap (similar as in Section 3.3.1, which will be called 'correlation coefficient' from here on). Two fully overlapping probability density functions would give a value for the correlation coefficient of 1, whereas 0 means no overlap at all. This analysis is made using a sliding 100 m window which is moved progressively along the

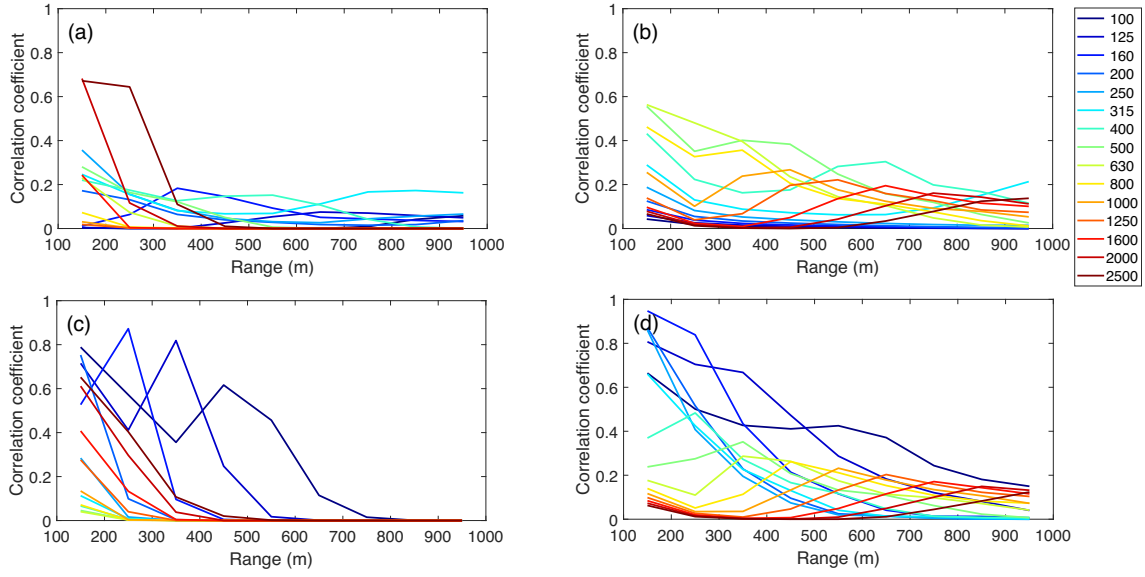


**Fig. 12.** The correlation coefficient between the PDF predicted for sound propagation in a refracting turbulent atmosphere and neglecting meteorological influences. In (a) and (b), rigid ground is modelled, in (c) and (d) the softer ground. In (a) and (c), fully downwardly refracting conditions are selected ($a_{log} > 0$, $a_{lin} > 0$), in (b) and (d) fully upwardly refracting atmospheres ($a_{log} < 0$, $a_{lin} < 0$). A correlation coefficient of 1 means fully overlapping distribution between the meteo and no meteo case, a value of 0 no overlap at all. The receiver height is 1.55 m.

100 to 1000 m range to estimate the range-dependent similarity between the 'no meteo case' and 'meteo case' PDFs for 9 range intervals with the middle points between 150 and 950 m, in steps of 100 m. The 'meteo case' PDFs include all the predicted levels in a given range interval for all possible combinations of $a_{log}$ and $a_{lin}$ for a given quadrant in Fig. 1, including turbulent scattering.

The results of this analysis are presented in Fig. 12 for sound propagation in the presence of the hard and soft ground, in combination with either fully upwardly or fully downwardly refracting atmospheres.

The presented graphs in Fig. 12 suggest that in the case of sound propagation in the atmosphere with downward refraction, the ground has a strong effect on the range-dependent meteo/no-meteo similarity. This is an expected result, as multiple reflection points on the ground could be identified in such atmospheres, especially during stronger refraction (see e.g. Ref. [6,11]). In the case of the rigid ground (see Fig. 12 (a)) and at the higher end of the frequency spectrum the similarity between the 'no meteo' and 'meteo' case reduces considerably beyond 200–300 m range. At low and mid frequencies, there is hardly any similarity, even at very short range.

In the case of sound propagation over soft ground and at frequencies up to 160 Hz there is a strong similarity between the 'no meteo' and 'meteo' case which extends up to 500 m (see Fig. 12 (c)). This suggests that sound propagation under downward refraction from sources operating at these frequencies can be predicted with a relatively simple model which does not need to include complex atmospheric effects up to this range. At higher sound frequencies, the similarity drops much faster. At the mid frequencies, similar to the rigid ground case, there is hardly any similarity even for the shortest range classes considered.

Similar conclusion can be made when the atmosphere is upward refracting (see Fig. 12 (b) and (d)). For rigid grounds, similarities between meteo/no-meteo are overall somewhat lower than for soft grounds, especially in the lower frequency range. The highest similarities are seen for soft ground and low frequencies at short range.

Mainly in the higher frequency range, the correlation coefficient does not necessarily decrease with range; however, correlation coefficients between meteo/no-meteo above 500 m stay low (less than 0.2).

## 4. Conclusions

This work, via numerical simulations, has studied the uncertainties in sound propagation over a flat impedance ground caused by the atmospheric effects and ground type. A main novelty of this work is that it has predicted and analysed the probability density functions for 1/3 octave bands, including the difference between sound pressure level in the absence ('no-meteo' case) and presence of atmospheric refraction and turbulence scattering ('meteo' case).

It has been found that downward refraction tends to lead to multi-peaked PDFs. The position and width of these peaks depend on the frequency of sound and ground type. At lower frequencies, e.g. below 250 Hz, these distributions peak near + 10 dB, which is due to the constructive interference, i.e. when multiple sound paths arrive at a single spot. At the higher frequencies, a distinct peak in the distribution near 0 dB is observed but becomes wider in the case of a softer ground. The effect of turbulent scattering has been found relatively small in this case.

The statistics for the sound pressure levels in the case of upward refraction has been found markedly different. Sound propagation in this atmosphere is affected strongly by turbulent scattering and less by the ground conditions, as is well known from existing literature [1,6,14]. At sound frequencies above 500 Hz the probability density functions predicted are close to the Gaussian distribution with a maximum being near −20 dB when expressing sound pressure levels relative to free field propagation.

Another novelty of this work is the study of the threshold in the atmospheric conditions beyond which the probability density function becomes markedly different from that predicted for non-refracting non-turbulent atmospheres. It has been found that for some atmospheric conditions and impedance grounds the statistics in sound propagation in the presence and absence of atmospheric effects are similar for some frequency ranges when drawing distributions over the full propagation range considered (up to 1 km). On the other hand, for other frequency bands and ground types, a considerable difference occurs even for moderate refraction. In particular, in the case of upward refraction there are close similarities between the PDFs predicted for the 'meteo' and 'no-meteo' cases in the presence of hard ground. For these conditions a relatively large difference between the two cases is never reached for sound propagation in a relatively broad frequency range of 400–1600 Hz up to a propagation distance of 1 km. These similarities have also been found as pronounced in the case of sound propagation in upward refracting atmospheres in the presence of soft ground.

Finally, this work is novel because it has studied the range-dependent similarities between 'no meteo' and 'meteo' cases. It was found that for sound propagation in a downward refracting atmosphere, the ground and propagation range have a very strong effect on the PDF. Predicted high similarities, observed at a few 1/3 octave bands at short range, drop rapidly once a propagation distance of 300–500 m is reached. For most frequencies, such similarities are very limited at any range. This suggests that sound propagation under these conditions cannot be predicted with a model which does not include complex atmospheric effects. In case of upward refraction, similarities with the 'no-meteo' case are overall slightly higher, but rather similar conclusions can be drawn.

The main significance of this work is that it provides a foundation for the right choice of a model which can be used to predict sound propagation in a computationally efficient and accurate way for a given set of meteorological conditions. This is particularly important for applications related to sound localisation and characterisation which require the knowledge of statistics associated with propagation uncertainties.

Some limitations of the current work need to be reported. Example statistics are drawn here based on a highly detailed meteorological dataset for a single location only. The statistics drawn here are not necessarily representative for all possible locations and atmospheric conditions. Although the shapes of the distributions might change at other locations, the extent to which meteorological influences can be neglected, as discussed in Section 3, are expected to have a much wider applicability than just for one site.

The turbulence scattering approach used here is approximate but it avoids blowing up computational cost when explicitly modelling a representative set of turbulent realisations for each meteorological condition. Although the range and qualitative behaviour of predicted sound pressure levels in strong upward refracting conditions fit experimental findings, an accurate description of turbulent scattering of sound waves under any atmospheric condition is not guaranteed.

## Declaration of Competing Interest

The authors declare that they have no known competing financial interests or personal relationships that could have appeared to influence the work reported in this paper.

## Acknowledgements

The authors acknowledge the support of Defence Science and Technology Laboratory (Dstl) UK and EPSRC CASE studentship award to the University of Sheffield. The authors also acknowledge some support to this work from the EPSRC Grant EP/R022275/1.

## References

[1] Attenborough K, Li KM, Horoshenkov KV. Predicting Outdoor Sound. CRC Press; 2006.
[2] Wilson DK, Pettit CL, Ostashev VE, Vecherin SN. Description and quantification of uncertainty in outdoor sound propagation calculations. J. Acoust. Soc. Am. 2014;136:1013–28.
[3] Ostashev VE, Wilson DK. Statistical characterization of sound propagation over vertical and slanted paths in a turbulent atmosphere. Acta Acust. united Ac. 2018;104:571–85.
[4] Yokota T., Makino K., Iizumi G., Tsutsumi T. Long-term experiments on influences of ground surface and meteorological conditions on outdoor sound propagation using an unattended impulse response measurement system. Proc. 49th int. congress and exposition on noise control eng./Internoise 2020; Seoul, South Korea.
[5] Parry JA, Horoshenkov KV, Williams DP. Investigating uncertain geometries effect on sound propagation in a homogeneous and non-moving atmosphere over an impedance ground. Appl. Acoust. 2020;160:107122.
[6] Salomons E. Computational Atmospheric Acoustics. Dordrecht, The Netherlands: Kluwer; 2001.
[7] L'Espérance A, Nicolas J, Wilson DK, Thomson DW, Gabillet Y, Daigle G. Sound propagation in the atmospheric surface layer: Comparison of experiment with FFP predictions. Appl. Acoust. 1993;40:325–46.
[8] Swearingen ME, Horvath R, White MJ. Climate analysis for noise assessment. Appl. Acoust. 2017;119:50–6.
[9] Van Renterghem T, Botteldooren D. Variability due to short-distance favorable sound propagation and its consequences for immission assessment. J. Acoust. Soc. Am. 2018;143:3406–17.
[10] Heimann D, Bakermans M, Defrance J, Kühner D. Vertical sound speed profiles determined from meteorological measurements near the ground. Acta Acust. United Ac. 2007;93:228–40.
[11] Heimann D, Salomons EM. Testing meteorological classifications for the prediction of long-term average sound levels. Appl. Acoust. 2004;65:925–50.
[12] Cooper JL, Swanson DC. Parameter selection in the Green's function parabolic equation. Appl. Acoust. 2007;68:390–402.
[13] ERA5 database : https://www.ecmwf.int/en/forecasts/datasets/reanalysis-datasets/era5
[14] Ostashev VE, Wilson DK. Acoustics in Moving Inhomogeneous Media. second ed. Boca Raton, London: CRC Press, Taylor and Francis; 2016.
[15] Ostashev VE, Wilson DK. Relative contributions from temperature and wind velocity fluctuations to the statistical moments of a sound field in a turbulent atmosphere. Acust. Acta Acust. 2000;86:260–8.
[16] Forssén J. Influence of Atmospheric Turbulence on Sound Reduction by a Thin, Hard Screen: A Parameter Study Using the Sound Scattering Cross-section, Proc. Long Range Sound Propagation Symp. USA: Jackson; 1998.
[17] van Maercke D, Defrance J. Development of an Analytical Model for Outdoor Sound Propagation Within the Harmonoise Project. Acta Acust. united Ac. 2007;93:201–12.
[18] Chevret P, Blanc-Benon P, Juvé D. A numerical model for sound propagation through a turbulent atmosphere near the ground. J. Acoust. Soc. Am. 1996;100:3587–99.
[19] Lam YW. An analytical model for turbulence scattered rays in the shadow zone for outdoor sound propagation calculation. J. Acoust. Soc. Am. 2009;125:1340–50.
[20] Gilbert KE, Raspet R, Di X. Calculation of turbulence effects in an upward-refracting atmosphere. J. Acoust. Soc. Am. 1990;87:2428–37.
[21] Cheinet S. A numerical approach to sound levels in near-surface refractive shadows. J. Acoust. Soc. Am. 2012;131:1946–58.
[22] Horoshenkov KV, Hurrell A, Groby J-P. A three-parameter analytical model for the acoustical properties of porous media. J. Acoust. Soc. Am. 2019;145:2512–7.
[23] Supplementary material available online: https://drive.google.com/drive/folders/1Uxqwh2Imc_Jx-JnlS8eycVvyQqZXMfX5?usp=sharing